Journal of Nuclear Medicine, published on March 6, 2025 as doi:10.2967/jnumed.124.268943

Differences in Fibroinflammatory Activity Shown on ^{68}Ga-FAPI-04 and ^{18}F-FDG PET/CT in the Two Subtypes of IgG4-Related Disease

Silu Liu[1,2], Qingqing Pan[1], Hongzhe Zhang[1], Linyi Peng[3], Wen Zhang[3], YunLu Feng[4], Dong Wu[4], and Yaping Luo[1,2]

[1]*Department of Nuclear Medicine, Chinese Academy of Medical Sciences and Peking Union Medical College Hospital, Beijing, China;* [2]*State Key Laboratory of Common Mechanism Research for Major Diseases, Beijing, China;* [3]*Department of Rheumatology and Clinical Immunology, Chinese Academy of Medical Sciences and Peking Union Medical College Hospital, Beijing, China; and* [4]*Department of Gastroenterology, Chinese Academy of Medical Sciences and Peking Union Medical College Hospital, Beijing, China*

IgG4-related disease (IgG4-RD) is a highly heterogeneous autoimmune disease. Recently, 2 subtypes of IgG4-RD, proliferative and fibrotic, were defined according to patients' clinicopathologic characteristics. The purpose of this study was to determine the difference in fibroinflammatory activity shown on ^{68}Ga-FAPI-04 and ^{18}F-FDG PET/CT in the proliferative and fibrotic IgG4-RD subtypes. **Methods:** Thirty-seven newly diagnosed IgG4-RD patients (29 of the proliferative subtype and 8 of the fibrotic subtype) who had undergone ^{68}Ga-FAPI-04 and ^{18}F-FDG PET/CT were enrolled. SUV_{max} and target-to-background ratio (TBR) of IgG4-RD lesions were measured. To evaluate the weight of fibroinflammatory activity, the PET index of a lesion was calculated as the quotient of SUV_{max} or TBR of ^{68}Ga-FAPI-04 and that of ^{18}F-FDG. For the assessment of the global disease in an individual patient, the PET index was defined as the ratio of SUV_{mean} of all involved lesions in ^{68}Ga-FAPI-04 PET/CT to that in ^{18}F-FDG. **Results:** The ^{18}F-FDG uptake values of the most prominent lesions in the proliferative and fibrotic subtypes were similar; however, the proliferative subtype showed significantly higher uptake of ^{68}Ga-FAPI-04 than did the fibrotic subtype (SUV_{max}, 17.67 ± 7.46 vs. 10.93 ± 2.22, $P = 0.005$; TBR, 15.49 ± 8.23 vs. 9.25 ± 3.00, $P = 0.015$). The PET index of proliferative-subtype patients was higher than that of fibrotic-subtype patients (1.46 ± 0.41 vs. 1.14 ± 0.39, $P = 0.039$). The PET index of pancreatobiliary disease was significantly higher than that of head-and-neck disease, fibrosis or aortitis, lymph nodes, and another disease subtype ($P < 0.05$). After first-line treatment, patients with a PET index of at least 1.5 had significantly shorter relapse-free survival than those with a PET index of less than 1.5 (22.0 mo vs. not reached, $P < 0.0001$; hazard ratio, 13.46; 95% CI, 2.236–81.03). **Conclusion:** The proliferative subtype of IgG4-RD had a greater weight of fibroinflammatory activity than that of the fibrotic subtype. The PET index, a marker of the weight of fibroinflammatory activity, is predictive of relapse-free survival of IgG4-RD.

Key Words: IgG4-related disease; proliferative subtype; fibrotic subtype; ^{68}Ga-FAPI-04; ^{18}F-FDG

J Nucl Med 2025; 00:1–7
DOI: 10.2967/jnumed.124.268943

IgG4-related disease (IgG4-RD) is a fibroinflammatory disease involving nearly every organ system. The most affected organs of IgG4-RD are the lacrimal gland, salivary gland, lung, paravertebral soft tissue, pancreas, bile duct tree, kidney, retroperitoneum, aorta, meninges, and thyroid gland (*1*). Imaging examination plays an important role in the diagnosis and evaluation of IgG4-RD, and more than half of patients have involvement in 5 or 6 organs (*2*). Recently, fibroblast activation protein–targeted PET imaging with ^{68}Ga-labeled agents was introduced in clinical studies of both tumors and inflammatory disease, such as IgG4-RD, rheumatoid arthritis, Crohn disease, and renal fibrosis (*3–8*). In our previous study of IgG4-RD (*6*), we found that IgG4-RD could be imaged with ^{68}Ga-FAPI-04 PET/CT, because storiform fibrosis constitutes its key histopathologic feature (*9*). Furthermore, we found that ^{68}Ga-FAPI-04 had a higher positive rate and higher uptake values than ^{18}F-FDG in the pancreas, bile duct or liver, and salivary gland; conversely, lymph node disease was ^{18}F-FDG-avid but did not accumulate ^{68}Ga-FAPI-04. The observed variability in the uptake patterns across different involved organs indicates heterogeneous histopathologic and molecular features in IgG4-RD.

Recently, IgG4-RD has been divided into 2 subtypes, proliferative and fibrotic, according to the clinicopathologic characteristics of patients (*2*). The clinical manifestations, treatment response, and prognosis vary greatly between the subtypes of patients. Proliferative IgG4-RD shows high levels of serum IgG4 and IgE, has high eosinophil counts, and usually involves multiple organs, including the lacrimal gland, salivary gland, pancreas, bile duct, lung, and lymph nodes. The fibrotic subtype commonly affects the retroperitoneum, aorta or periaortic tissue, mesentery, pachymeninx, and thyroid, with normal or slightly elevated serum IgG4 and IgE levels and eosinophil counts (*10*). Histopathologically, the 2 subtypes of disease show different levels in IgG4-positive cell infiltration, germinal center, and storiform fibrosis (*9*). The treatment response to glucocorticoid also varies between the subtypes of patients: definite response to glucocorticoids is reliably applied only to the proliferative subtype, whereas improvement of fibrotic disease after glucocorticoid treatment is not obvious (*11*).

It has been reported that a combination of ^{68}Ga-FAPI-04 and ^{18}F-FDG PET/CT could discriminate between inflammatory and fibrotic activity in IgG4-RD. ^{18}F-FDG PET–positive lesions showed dense lymphoplasmacytic infiltration of IgG4-positive cells in histology, whereas ^{68}Ga-FAPI-04 PET–positive lesions showed abundant activated fibroblasts expressing fibroblast activation protein (*12*).

Received Oct. 10, 2024; revision accepted Feb. 10, 2025.
For correspondence or reprints, contact Yaping Luo (luoyaping@live.com).
Published online Mar. 6, 2025.
COPYRIGHT © 2025 by the Society of Nuclear Medicine and Molecular Imaging.

In this study, we aimed to investigate whether there was difference in the weight of fibrosis, as shown by ^{68}Ga-FAPI-04, and inflammation, as shown by ^{18}F-FDG, in the different subtypes of IgG4-RD and in organ involvement.

MATERIALS AND METHODS

Study Design and Patients

This is a retrospective analysis of the data from our prospective cohort study on ^{68}Ga-FAPI-04 PET/CT in evaluation of IgG4-RD (NCT 04125511). The study was approved by the institutional review board of Peking Union Medical College Hospital (protocol ZS-1810), and written informed consent was obtained from each patient. We reviewed all recruited patients from November 2019 to July 2024 and selected newly diagnosed IgG4-RD patients with the following inclusion criteria: patients fulfilled the 2019 American College of Rheumatology–European League Against Rheumatism classification criteria for IgG4-RD (specificity of 99.2% [95% CI, 97.2%–99.8%] and sensitivity of 85.5% [95% CI, 81.9%–88.5%] for diagnosis) (*13*); underwent both ^{68}Ga-FAPI-04 and ^{18}F-FDG PET/CT, which were performed within 2 wk; and did not receive treatment against IgG4-RD (e.g., glucocorticoids and immunosuppressants) before the PET/CT scans. Thus, 37 patients were included in the present study. The involved organs were classified as the proliferative or fibrotic subtype through a consensus review. The proliferative-subtype organs were the lymph node, lacrimal gland, salivary gland, pancreas, bile duct, kidney, lung, pituitary, and paranasal sinus, and the fibrotic-subtype organs were the retroperitoneum, aorta and periaortic tissue, mesentery, mediastinum, pachymeninges, and Riedel thyroiditis (*2*). Subsequently, patients were classified into 1 of the 2 categories, the proliferative or fibrotic subtype, based on the organs involved. In cases of overlap between of the subtypes in an individual patient, the patient's classification into an IgG4-RD subtype was determined by the predominant subtype of the involved organs and by serologic and clinical characteristics, as determined by senior rheumatologists (*2*). Clinical and follow-up data, including laboratory examinations, treatment, response, and relapse, were obtained from the medical record. The flowchart of patient enrollment is shown in Figure 1.

PET/CT Imaging

The DOTA-FAPI-04 peptide was purchased from CSBio. Radiolabeling of ^{68}Ga-FAPI-04 was performed manually before injection, according to previously published procedures (*6*). ^{18}F-FDG was synthesized with ^{18}F produced by an 11-MeV cyclotron (CTI RDS 111; Siemens). The PET/CT scans were performed on integrated PET/CT scanners (Biograph 64 TruePoint TrueV; Siemens; and Polestar m660; SinoUnion), with an uptake time of 73.8 ± 23.4 min for ^{18}F-FDG and 53.9 ± 16.6 min for ^{68}Ga-FAPI-04.

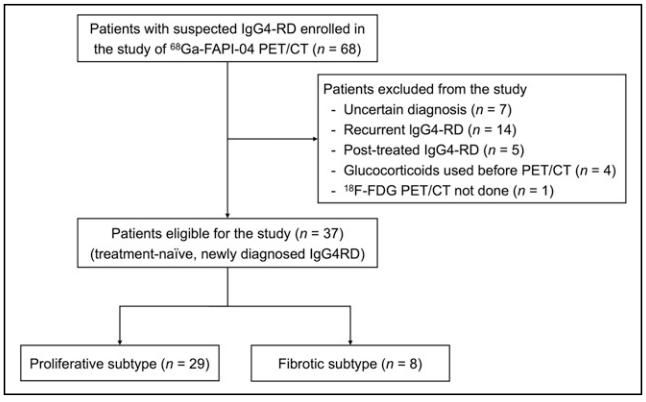

FIGURE 1. Flowchart of patient enrollment.

Image Interpretation and Semiquantitative Measurements

^{18}F-FDG and ^{68}Ga-FAPI-04 PET/CT scans were viewed on the Syngo multimodality workplace (Siemens) and assessed by 2 experienced nuclear medicine physicians (with >10 y of experience in PET/CT), with consensus for the image interpretation of organ involvement. SUV_{max} of the lesion exhibiting the greatest uptake in each involved organ and the blood pool background (measured in the descending aorta, 1-cm diameter) were measured by the same nuclear medicine physician using the volume-of-interest method with a unified standard. Each involved organ was also assessed using the target-to-background ratio (TBR), which was defined as SUV_{max} of the lesion with the greatest uptake divided by SUV_{max} of the blood pool background.

To further evaluate the weight of fibrosis (shown by ^{68}Ga-FAPI-04) and inflammation (shown by ^{18}F-FDG) in a certain lesion or involved organ, the parameter of the PET index was established, which was defined as the quotient of SUV_{max} or TBR of ^{68}Ga-FAPI-04 and SUV_{max} or TBR of ^{18}F-FDG in the involved organ or lesion. For the assessment of global disease in an individual patient, the PET index was calculated as the ratio of SUV_{mean} of all involved lesions in ^{68}Ga-FAPI-04 to SUV_{mean} of all lesions in ^{18}F-FDG. To measure SUV_{mean} of global lesions, metabolic lesion volume (MLV, defined as the sum of the metabolic volumes of all involved lesions) and total lesion uptake (TLU, defined as the sum of an individual MLV multiplied by its SUV_{mean}) were semiautomatically measured with the MIM workstation (version 6.6.11; MIM Software). Volumes of interest were drawn that included all involved lesions previously located by the 2 readers in the PET/CT images. Subsequently, the contours were semiautomatically segmented with an SUV cutoff of 2.5 and were then checked and manually adjusted to exclude physiologic uptakes, such as the urinary tract and brain. Afterward, volumetric parameters of TLU and MLV were automatically obtained from the statistics generated with the final volumetric extraction, and SUV_{mean} of all involved lesions was calculated as the quotient of TLU and MLV (SUV_{mean}, TLU/MLV). Lymph node disease was excluded from MLV and TLU measurements, because its characteristics in PET/CT (non–^{68}Ga-FAPI-avid) are completely different from those of other involved organs, as we previously published (*6*).

Statistical Analysis

Statistical analyses were done with SPSS Statistics software (version 26.0; IBM) and GraphPad Prism (version 10.2.1; GraphPad Software). The correlation between immunohistochemical staining of IgG4 and SUV_{max} of the biopsied organs was analyzed using the Spearman rank test. Clinical characteristics between proliferative-subtype and fibrotic-subtype patients were compared using the Student *t* test (data with normal distribution) or Wilcoxon test (skewed data, with the Shapiro–Wilk test for normality). PET/CT measurements of the involved lesions between ^{68}Ga-FAPI-04 and ^{18}F-FDG were compared using the paired *t* test (data with normal distribution) or paired Wilcoxon test (skewed data). The Kruskal–Wallis test was used to compare the PET/CT measurements among the 3 clusters of involved organs, and the Bonferroni adjustment was performed to control the false positivity of multiple comparisons. The PET index between the 2 subtypes of patients was compared using the Student *t* test. The Kaplan–Meier method was used to estimate survival curves, which were compared by the log-rank test. A 2-tailed *P* value of less than 0.05 was regarded as statistically significant.

RESULTS

Clinical Characteristics

Thirty-seven patients with treatment-naïve, newly diagnosed IgG4-RD were included in the study (33 men and 4 women; age, 55.4 ± 14.1 y; range, 17–81 y). The median disease duration was 6.0 mo (range, 2 wk to 9 y). Eight patients had an allergy history (e.g., asthma and urticaria). Biopsy was done for diagnosis of

IgG4-RD in 28 patients; the biopsy sites were the pancreas ($n = 11$), salivary gland ($n = 7$), lacrimal gland ($n = 1$), lung ($n = 1$), gastrointestinal tract ($n = 2$), gallbladder ($n = 1$), retroperitoneal mass ($n = 1$), kidney ($n = 2$), and lymph nodes ($n = 5$). Immunohistochemical results were available for 22 patients, and IgG4-positive lymphoplasmacytes were identified in the specimens of 17 patients. Furthermore, the IgG4-positive–to–IgG-positive plasma cell ratio demonstrated a positive correlation with SUV_{max} of the biopsied organ on ^{18}F-FDG PET/CT ($r = 0.56$, $P = 0.025$). However, this correlation was not observed with ^{68}Ga-FAPI-04 PET/CT ($r = 0.141$, $P = 0.603$).

Twenty-nine patients were classified as the proliferative subtype, and 8 patients were classified as the fibrotic subtype. Comparison of the clinical characteristics of the 2 subtypes of IgG4-RD showed that serum IgG4 in the proliferative subtype was significantly higher than in the fibrotic subtype of patients (median, 14,400 mg/L; interquartile range, 7,553–30,950 mg/L; vs. median, 2,365 mg/L; interquartile range, 978–3,475 mg/L; $P = 0.000$). However, no statistical difference was found in C-reactive protein, IgE, eosinophil counts, or complement C3 or C4 levels between the proliferative and the fibrotic subtypes (Table 1).

Comparison of ^{68}Ga-FAPI-04 and ^{18}F-FDG PET/CT in Involved Organs

In the 37 recruited patients, the most commonly affected organs included the pancreas (28/37, 75.7%), salivary gland (25/37, 67.6%), lymph nodes (22/37, 59.5%), lacrimal gland or orbit (17/37, 45.9%), retroperitoneal or mediastinal fibrosis or periaortitis (16/37, 43.2%, including the pleura, pericardium, and mesentery), bile duct or liver (12/37, 32.4%), prostate or seminal vesicle (13/37, 35.1%), lung (11/37, 29.7%), and kidney (6/37, 16.2%). SUV_{max} of the matched lesions in the pancreas, submandibular gland, bile duct or liver, and fibrosis or periaortitis were significantly higher on ^{68}Ga-FAPI-04 than on ^{18}F-FDG PET/CT (paired Student t test, $P < 0.05$; Table 2). Moreover, with the benefit of lower background uptake with ^{68}Ga-FAPI-04, the TBR of the matched lesions was significantly higher on ^{68}Ga-FAPI-04 than on ^{18}F-FDG PET/CT in almost all involved organs except the lung and kidney (paired Student t test, $P < 0.05$; Table 2). Conversely, SUV_{max} and TBR of lymph nodes on ^{18}F-FDG PET/CT were significantly higher than on ^{68}Ga-FAPI-04 PET/CT (paired t test, $P < 0.01$; Table 2).

PET/CT Comparison Between Proliferative and Fibrotic Subtypes

Patient-Based Analysis. In the comparison of the PET/CT features between the proliferative and the fibrotic subtypes of IgG4-RD patients, the lesions with the greatest uptake in the 2 subtypes of patients showed similar ^{18}F-FDG uptake (SUV_{max}, 6.83 ± 2.49 vs. 7.56 ± 3.91, $P = 0.626$; TBR, 3.86 ± 1.55 vs. 4.38 ± 2.74, $P = 0.626$; Fig. 2); however, the proliferative subtype of patients showed significantly higher SUV_{max} and TBR of the most prominent lesions on ^{68}Ga-FAPI-04 PET/CT than did the fibrotic subtype of patients (SUV_{max}, 17.67 ± 7.46 vs. 10.93 ± 2.22, $P = 0.005$; TBR, 15.49 ± 8.23 vs. 9.25 ± 3.00, $P = 0.015$; Fig. 2). Furthermore, the PET index (where the PET index [patient-based] is the ratio of SUV_{mean} of global lesions in ^{68}Ga-FAPI-04 to SUV_{mean} of global lesions in ^{18}F-FDG) of the proliferative subtype was significantly higher than the PET index of the fibrotic subtype (1.46 ± 0.41 vs. 1.14 ± 0.39, $P = 0.039$; Fig. 2), suggesting more dominant uptake of ^{68}Ga-FAPI-04 in the proliferative subtype of IgG4-RD than in the fibrotic subtype.

Organ-Based Analysis. For further analysis of the contribution of fibrosis and inflammation to IgG4-RD involvement, we grouped the lesions, according to the involved organs, into 5 clusters (*14*): pancreatohepatobiliary disease, head-and-neck disease (Mikulicz disease), fibrosis or periaortitis (including the pleura, pericardium, and mesentery), lymph nodes, and others (including the lung, kidney, and prostate or seminal vesicle). We found that the PET index (where the PET index [lesion-based] is the quotient of SUV_{max} or TBR in ^{68}Ga-FAPI-04 and SUV_{max} or TBR in ^{18}F-FDG) of pancreatohepatobiliary disease was significantly higher than that of head-and-neck disease, fibrosis or periaortitis disease, and other types of disease ($P < 0.05$; Fig. 3). Moreover, the PET index of lymph node disease was significantly lower than that of all other disease subtypes ($P < 0.01$; Fig. 3). Examples of maximum-intensity projections of the dual-tracer PET scans of the proliferative and fibrotic subtypes of patients are shown in Figure 4.

PET/CT Characteristics in Predicting Relapse-Free Survival

After PET/CT evaluation, all patients were treated with glucocorticoids alone or glucocorticoids plus immunosuppressants against IgG4-RD. After a median follow-up of 45.3 mo (range, 1.0–63.0 mo),

TABLE 1
Comparison of Clinical Features Between Proliferative Subtype and Fibrotic Subtype

Feature	Proliferative subtype	Fibrotic subtype	*P*
n	29	8	
Sex	27 men and 2 women	6 men and 2 women	0.198
Age (y)	58.4 ± 11.9	44.6 ± 17.0	0.06
Serum IgG4 (mg/L)	14,400 (7,553–30,950)	2,365 (978–3,475)	0.000*
C-reactive protein (mg/L)	3.44 (1.10–14.98)	7.12 (3.33–9.84)	0.285
Serum IgE (KU/L)†	408 (209.75–889.5)	180 (56.8–511)	0.202
Eosinophils ($\times 10^9$/L)	0.32 (0.12–0.575)	0.22 (0.16–0.40)	0.121
Complement C3 (g/L)†	0.92 ± 0.45	1.15 ± 0.45	0.234
Complement C4 (g/L)†	0.15 ± 0.10	0.24 ± 0.14	0.065

*Statistically significant.
†Data not available for some patients.
Data are mean ± SD or median followed by interquartile range in parentheses.

TABLE 2
SUV_{max} and TBR of IgG4-RD Involvement in ^{68}Ga-FAPI-04 and ^{18}F-FDG PET/CT

Involved organ	*n*	SUV_{max}			TBR		
		^{68}Ga-FAPI-04	^{18}F-FDG	*P*	^{68}Ga-FAPI-04	^{18}F-FDG	*P*
Lacrimal gland or orbit	17	4.93 ± 2.11	4.50 ± 2.64	0.612	4.78 ± 2.68	2.48 ± 1.51	0.010*
Parotid gland	9	5.04 ± 3.12	4.38 ± 1.94	0.493	4.22 ± 1.72	2.60 ± 1.06	0.018*
Submandibular gland	25	8.22 ± 3.64	4.81 ± 2.07	0.000*	7.03 ± 3.33	2.74 ± 1.29	0.000*
Sublingual gland	13	6.68 ± 2.62	4.44 ± 1.73	0.050	6.56 ± 3.88	2.47 ± 1.18	0.004*
Lung	11	4.76 ± 2.88	4.06 ± 1.67	0.406	4.34 ± 2.66	2.57 ± 0.98	0.110
Pancreas	28	17.74 ± 7.82	4.61 ± 2.03	0.000*	15.80 ± 8.50	2.54 ± 1.15	0.000*
Bile duct or liver	12	7.28 ± 2.30	3.81 ± 1.02	0.000*	6.61 ± 2.61	2.13 ± 0.57	0.002*
Fibrosis or periaortitis	16	9.40 ± 4.09	6.64 ± 3.28	0.022*	7.88 ± 3.47	3.84 ± 2.15	0.001*
Kidney	6	6.75 ± 2.46	4.75 ± 0.61	0.170	6.38 ± 2.92	2.13 ± 0.59	0.065
Prostate or seminal vesicle	13	5.66 ± 1.81	6.21 ± 2.03	0.536	4.83 ± 1.44	3.42 ± 1.43	0.049*
Lymph node	22	2.03 ± 1.60	6.31 ± 2.19	0.000*	1.83 ± 1.87	3.58 ± 1.37	0.002*

*Statistically significant.
Data are number or mean ± SD.

8 patients experienced clinical relapse of disease (e.g., recurrence of abdominal pain, jaundice, elevation of pancreatic enzyme, hydronephrosis, and progression in imaging), so reinitiation of therapy or increased dose of medication was required (median relapse-free survival, 21.8 mo; range, 4.8–42.8 mo). The relapse-free survival curves did not show a significant difference between proliferative and fibrotic patients ($P = 0.607$; Fig. 5A), but for patients with a PET index of at least 1.5, relapse-free survival was significantly shorter than it was for patients with a PET index of less than 1.5 (estimated median relapse-free survival, 22.0 mo vs. not reached, $P < 0.0001$; hazard ratio, 13.46 [95% CI, 2.24–81.03]; Fig. 5B).

DISCUSSION

Consistent with our previous report (*6*), the current study on newly diagnosed IgG4-RD showed that SUV_{max} of IgG4-RD involvement in the submandibular gland, pancreas, bile duct or liver, and fibrosis or periaortitis was significantly higher on ^{68}Ga-FAPI-04 than on ^{18}F-FDG PET/CT. Moreover, the lower background uptake of ^{68}Ga-FAPI-04 contributed to increased TBR in more involved organs compared with TBR of ^{18}F-FDG, which may benefit the detection of disease and staging of IgG4-RD. We found that the proliferative and fibrotic subtypes of IgG4-RD patients showed distinct PET/CT characteristics: patients with proliferative-subtype disease showed significantly higher uptake of ^{68}Ga-FAPI-04 and a higher PET index (where the PET index is the ratio of SUV_{mean} of global lesions in ^{68}Ga-FAPI-04 to SUV_{mean} of global lesions in ^{18}F-FDG) than those with the fibrotic subtype; however, ^{18}F-FDG activity of the 2 subtypes was similar. A previous study reported that ^{68}Ga-FAPI-04 PET/CT permits the discrimination of inflammatory from fibrotic activity in IgG4-RD (*12*). Therefore, our findings suggested that patients with proliferative and fibrotic subtypes had comparative degrees of inflammation but that the weight of fibrosis was more dominant in the proliferative subtype than in the fibrotic subtype. Furthermore, we found that pancreatohepatobiliary disease, which is a major presentation in most proliferative IgG4-RD, provided more contribution than other involved organs to a higher PET index ($P < 0.05$).

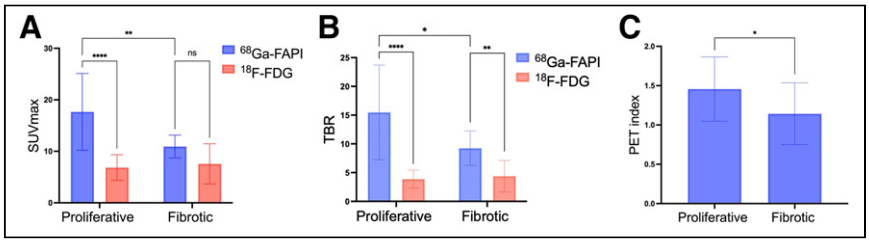

FIGURE 2. Comparison of PET/CT measurements between proliferative-subtype and fibrotic-subtype patients. (A and B) SUV_{max} (A) and TBR (B) of most prominent lesions on ^{68}Ga-FAPI-04 PET/CT were significantly higher in patients with proliferative subtype than in fibrotic-subtype patients (SUV_{max}, 17.67 ± 7.46 vs. 10.93 ± 2.22, $P = 0.005$; TBR, 15.49 ± 8.23 vs. 9.25 ± 3.00, $P = 0.015$). On ^{18}F-FDG PET/CT, there was no statistical difference of SUV_{max} and TBR between patients with proliferative subtype and those with fibrotic subtype (SUV_{max}, 6.83 ± 2.49 vs. 7.56 ± 3.91, $P = 0.626$; TBR, 3.86 ± 1.55 vs. 4.38 ± 2.74, $P = 0.626$). (C) PET index of patients with proliferative subtype was significantly higher than that of fibrotic-subtype patients (1.46 ± 0.41 vs. 1.14 ± 0.39, $P = 0.039$). TBR is ratio of SUV_{max} of lesion to SUV_{max} of blood pool. PET index (patient-based) is ratio of SUV_{mean} of global lesions in ^{68}Ga-FAPI-04 to SUV_{mean} of global lesions in ^{18}F-FDG. ns = not significant. *$P < 0.05$. **$P < 0.01$. ****$P < 0.0001$.

Histopathologically, storiform fibrosis in both the proliferative subtype and the fibrotic subtype is commonly seen; however, the proliferative subtype is more prominent in the infiltration of lymphoid plasma cells and formation of germinal centers, whereas the fibrotic subtype has more common obliterative phlebitis with sparse lymphoplasmacytic infiltration (*2*,*15*). Both the proliferative subtype and the fibrotic subtype showed intense uptake of ^{68}Ga-FAPI-04, which is a reflection of fibrosis. More importantly, the observation of a significantly greater weight of fibrosis in the proliferative subtype

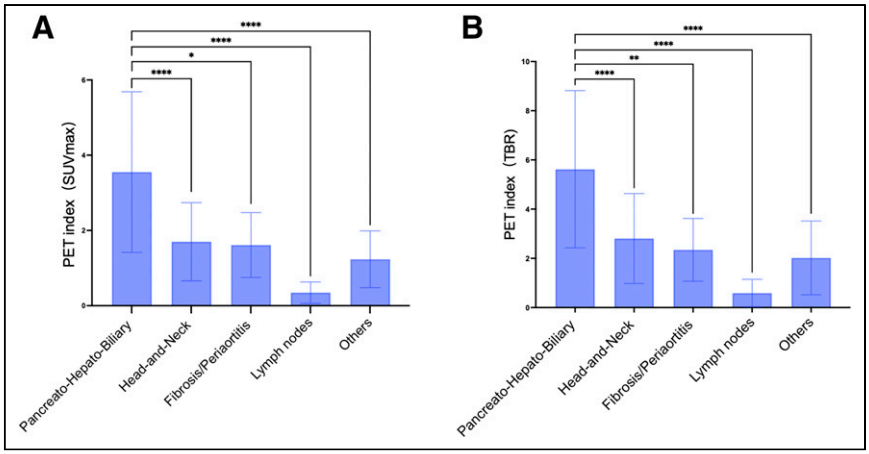

FIGURE 3. Comparison of PET index among pancreatohepatobiliary disease, head-and-neck disease, fibrosis or periaortitis, lymph nodes, and other disease. (A and B) PET index calculated by SUV_{max} (A) and TBR (B) of pancreatohepatobiliary disease was significantly higher than that of head-and-neck disease, fibrosis or periaortitis, lymph nodes, and other disease subtypes (PET index [calculated by SUV_{max}], 3.55 ± 2.11 vs. 1.70 ± 1.04, 1.61 ± 0.86, 0.35 ± 0.28, and 1.23 ± 0.76, respectively, $P < 0.05$; PET index [calculated by TBR], 5.62 ± 3.20 vs. 2.81 ± 1.83, 2.35 ± 1.24, 0.59 ± 0.56, and 2.02 ± 1.50, respectively, $P < 0.01$). PET index calculated by either SUV_{max} (A) or TBR (B) of lymph nodes was significantly lower than that of all other disease subtypes ($P < 0.01$). TBR is ratio of SUV_{max} of lesion to SUV_{max} of blood pool. PET index (lesion-based) is quotient of SUV_{max} or TBR in ^{68}Ga-FAPI-04 and SUV_{max} or TBR in ^{18}F-FDG. *$P < 0.05$. **$P < 0.01$. ****$P < 0.0001$.

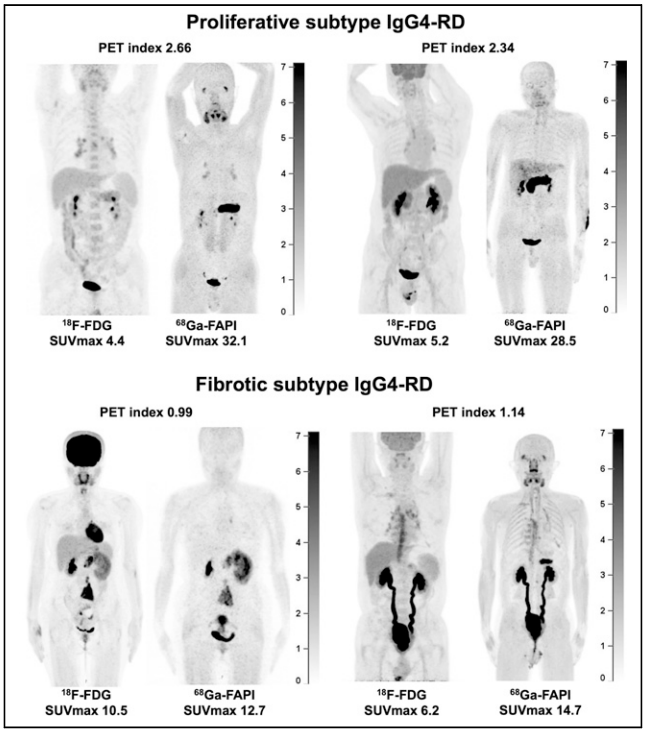

FIGURE 4. PET image examples of patients with proliferative subtype and fibrotic subtype of IgG4-RD. Patients with proliferative-subtype disease showed significantly higher uptake of ^{68}Ga-FAPI-04 than of ^{18}F-FDG in involved organs, whereas ^{68}Ga-FAPI-04 activity and ^{18}F-FDG activity in fibrotic-subtype disease was similar. PET index of proliferative-subtype patients was higher than that of fibrotic-subtype patients.

than in the fibrotic subtype is worth further exploration. We know that IgG4-RD is the continuous dynamic process of fibroinflammatory disease: it passes through stages of chronic proliferative inflammation and recurrent tissue damage and finally ends in tissue fibrosis. The proliferative and fibrotic subtypes represent the opposite ends of the continuum (*16*): the proliferative subtype reflects the inflammation and early fibrosis stage of IgG4-RD, and the fibrotic subtype reflects the end-stage scar of IgG4-RD. The fibrotic subtype is rich in fibroblasts, but most activated fibroblasts have been replaced by quiescent fibroblasts (*17*). This theory is supported by our results from PET/CT, because ^{68}Ga-FAPI-04 is expressed only in activated fibroblasts, not in quiescent fibrosis (*18*). Furthermore, the higher PET index (representing the fibroinflammatory weight) in the proliferative subtype, especially in pancreatohepatobiliary disease, indicates a higher proportion of activated fibroblasts, because it is an early fibrosis stage. In addition, it would be worthwhile to conduct further investigation into quiescent fibrotic disease and patients with high inflammatory activity or active fibrosis, as well as the impact on treatment response and disease relapse.

Glucocorticoids are the cornerstone of treatment for IgG4-RD, and patients typically respond well to this intervention (*2*). Patients with the proliferative subtype usually have an excellent response to glucocorticoids, whereas those with the fibrotic subtype have a weaker response (*19*). A higher PET index for the proliferative subtype than for the fibrotic subtype provided an explanation for the different responses of the 2 subtypes to glucocorticoids, because glucocorticoids exert their effects through the activation of glucocorticoid receptors, which are abundantly expressed in fibroblasts (*20*).

Despite a swift response to glucocorticoids, especially in pancreatohepatobiliary disease, disease flares are common at low doses or after tapering (*21*). A retrospective cohort study of 448 IgG4-RD patients treated with glucocorticoids alone or in combination with immunosuppressants revealed that patients with the fibrotic subtype were less likely to relapse than those with the proliferative subtype (*22*). In contrast, in our study, we did not find a significant difference in relapse-free survival between the proliferative and the fibrotic subtypes, possibly because of the small sample size. However, the PET index, which represented the weight of fibroinflammatory activity, was related to the relapse-free survival of newly diagnosed IgG4-RD patients after first-line treatment: patients with a PET index of at least 1.5 had significantly shorter relapse-free survival than patients with a PET index of less than 1.5 (estimated median relapse-free survival, 22.0 mo vs. not reached; $P < 0.0001$). It would be worthwhile to conduct prospective clinical trials to confirm the prognostic and predictive values of the PET index for IgG4-RD and to investigate its role in selection of medication (e.g., B-cell depletion and antifibrotic drugs), strategy of withdrawal of immunosuppressants and low-dose steroids, duration of maintenance treatment, etc.

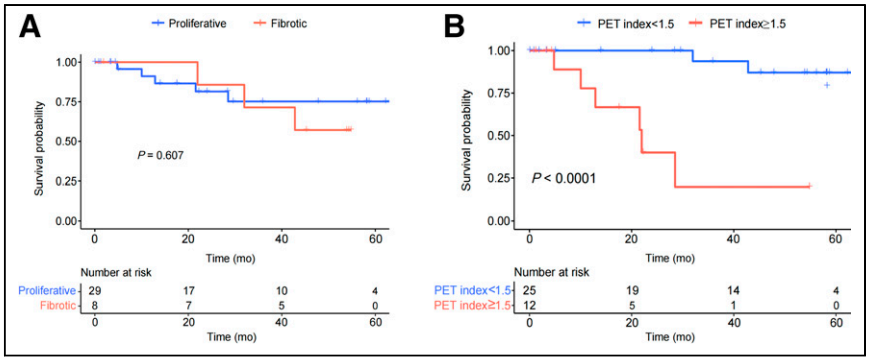

FIGURE 5. Kaplan–Meier curves of relapse-free survival for patients with proliferative subtype and fibrotic subtype (A; median relapse-free survival, not reached; $P = 0.607$) and for patients with PET index ≥ 1.5 and with PET index < 1.5 (B; median relapse-free survival, 22.0 mo [95% CI, 2.2–81.0 mo] vs. not reached; $P < 0.0001$). PET index (patient-based) is ratio of SUV_{mean} of global lesions in ^{68}Ga-FAPI-04 to SUV_{mean} of global lesions in ^{18}F-FDG.

The clinical characteristics of proliferative and fibrotic IgG4-RD are different. Patients with the proliferative subtype tend to have high serum concentrations of IgG4 and IgE, hypocomplementemia, peripheral eosinophilia, and high frequency of atopy history. By contrast, patients with the fibrotic subtype often have normal or mildly elevated serum IgG4 and IgE concentrations, show elevation of inflammatory markers such as erythrocyte sedimentation rate and C-reactive protein, are seldom hypocomplementemic, rarely have peripheral eosinophilia, and are less likely to show atopy (*16*,*17*,*22*). In our study, we consistently found that the serum IgG4 level of the proliferative subtype was significantly higher than that of the fibrotic subtype. However, there were no significant differences in eosinophil counts, C-reactive protein, complement C3 or C4, and IgE concentrations between the 2 subtypes, possibly because of the small sample size.

Our study has some limitations. First, as a pilot study on ^{68}Ga-FAPI-04 in IgG4-RD, the sample size was relatively small, especially for the fibrotic IgG4-RD cases, but the proportion of proliferative-subtype and fibrotic-subtype cases was consistent with another cohort study (*22*). Second, the retrospective study did not encompass the analysis of histopathologic features of fibrosis. However, we did analyze the immunohistochemical results of IgG4-positive cells and found that the IgG4-positive–to–IgG-positive plasma cell ratio demonstrated a positive correlation with SUV_{max} of the biopsied organ on ^{18}F-FDG PET/CT. However, such a correlation was not observed with ^{68}Ga-FAPI-04 PET/CT. This finding aligns with a prior study that revealed ^{18}F-FDG PET–positive lesions exhibited dense lymphoplasmacytic infiltration of IgG4-positive cells on histologic analysis, whereas ^{68}Ga-FAPI-04 PET–positive lesions demonstrated substantial activated fibroblast expression of fibroblast activation protein (*12*). Third, PET/CT scans were not repeated during or after treatment; therefore, we did not include treatment response assessment with PET/CT in the current study. Finally, the measurement of the PET index for an individual patient might be improved. The volumes of interest in ^{68}Ga-FAPI-04 and ^{18}F-FDG PET/CT were contoured according to metabolic activity. Therefore, the PET index might underestimate the authentic weight of fibroinflammatory activity, because some lesions were not hypermetabolic on ^{18}F-FDG PET/CT.

CONCLUSION

Our study demonstrated that ^{68}Ga-FAPI-04 is superior to ^{18}F-FDG PET/CT in detecting IgG4-RD in most affected organs. The proliferative subtype of IgG4-RD showed more dominant uptake of ^{68}Ga-FAPI-04 than did the fibrotic subtype, suggesting more activation of fibroblasts in proliferative IgG4-RD. The PET index, which is a measure of the weight of fibroinflammatory activity, is predictive of relapse-free survival in newly diagnosed IgG4-RD after first-line treatment with glucocorticoid-containing regimens.

DISCLOSURE

This work was supported by National High Level Hospital Clinical Research Funding (2022-PUMCH-B-070), the CAMS Innovation Fund for Medical Sciences (2024-I2M-C&T-B-034), and the National Natural Science Foundation of China (32370946). No other potential conflict of interest relevant to this article was reported.

KEY POINTS

QUESTION: Is there any difference of fibroinflammatory activity shown on ^{68}Ga-FAPI-04 and ^{18}F-FDG PET/CT between the proliferative and the fibrotic subtypes of IgG4-RD?

PERTINENT FINDINGS: In our cohort study of 37 patients with IgG4-RD, proliferative IgG4-RD showed more dominant uptake of ^{68}Ga-FAPI-04 than did the fibrotic subtype. The PET index, a marker of the weight of fibroinflammatory activity derived from ^{68}Ga-FAPI-04 and ^{18}F-FDG PET/CT, is predictive of relapse-free survival after first-line treatment with glucocorticoid-containing regimens.

IMPLICATIONS FOR PATIENT CARE: Fibroinflammatory activity and PET/CT might constitute a promising biomarker in the classification of IgG4-RD and prediction of treatment outcomes.

REFERENCES

1. Katz G, Stone JH. Clinical perspectives on IgG4-related disease and its classification. *Annu Rev Med.* 2022;73:545–562.
2. Zhang W, Stone JH. Management of IgG4-related disease. *Lancet Rheumatol.* 2019;1:e55–e65.
3. Luo Y, Pan Q, Zhou Z, et al. ^{68}Ga-FAPI PET/CT for rheumatoid arthritis: a prospective study. *Radiology.* 2023;307:e222052.
4. Luo Y, Pan Q, Xu H, Zhang R, Li J, Li F. Active uptake of ^{68}Ga-FAPI in Crohn's disease but not in ulcerative colitis. *Eur J Nucl Med Mol Imaging.* 2021;48:1682–1683.
5. Pan Q, Luo Y, Zhang W. Idiopathic retroperitoneal fibrosis with intense uptake of ^{68}Ga-fibroblast activation protein inhibitor and ^{18}F-FDG. *Clin Nucl Med.* 2021;46:175–176.
6. Luo Y, Pan Q, Yang H, Peng L, Zhang W, Li F. Fibroblast activation protein-targeted PET/CT with ^{68}Ga-FAPI for imaging IgG4-related disease: comparison to ^{18}F-FDG PET/CT. *J Nucl Med.* 2021;62:266–271.
7. Chen L, Zhong X, Li L, et al. [^{68}Ga]Ga-FAPI-04 PET/CT on assessing Crohn's disease intestinal lesions. *Eur J Nucl Med Mol Imaging.* 2023;50:1360–1370.
8. Zhou Y, Yang X, Liu H, et al. Value of [^{68}Ga]Ga-FAPI-04 imaging in the diagnosis of renal fibrosis. *Eur J Nucl Med Mol Imaging.* 2021;48:3493–3501.

9. Deshpande V, Zen Y, Chan JK, et al. Consensus statement on the pathology of IgG4-related disease. *Mod Pathol.* 2012;25:1181–1192.
10. Peng Y, Li JQ, Zhang PP, et al. Clinical outcomes and predictive relapse factors of IgG4-related disease following treatment: a long-term cohort study. *J Intern Med.* 2019;286:542–552.
11. Khosroshahi A, Wallace ZS, Crowe JL, et al.; Second International Symposium on IgG4-Related Disease. International consensus guidance statement on the management and treatment of IgG4-related disease. *Arthritis Rheumatol.* 2015;67:1688–1699.
12. Schmidkonz C, Rauber S, Atzinger A, et al. Disentangling inflammatory from fibrotic disease activity by fibroblast activation protein imaging. *Ann Rheum Dis.* 2020;79:1485–1491.
13. Wallace ZS, Naden RP, Chari S, et al.; Members of the ACR/EULAR IgG4-RD Classification Criteria Working Group. The 2019 American College of Rheumatology/European League Against Rheumatism classification criteria for IgG4-related disease. *Ann Rheum Dis.* 2020;79:77–87.
14. Wallace ZS, Zhang Y, Perugino CA, Naden R, Choi HK, Stone JH; ACR/EULAR IgG4-RD Classification Criteria Committee. Clinical phenotypes of IgG4-related disease: an analysis of two international cross-sectional cohorts. *Ann Rheum Dis.* 2019;78:406–412.
15. Liao S, Zhang X, Zhu F, et al. Comparison of two subsets of Chinese patients with retroperitoneal fibrosis in terms of IgG4 immunohistochemical staining. *Rheumatology (Oxford).* 2019;58:455–462.
16. Katz G, Hernandez-Barco Y, Palumbo D, Guy TV, Dong L, Perugino CA. Proliferative features of IgG4-related disease. *Lancet Rheumatol.* 2024;6:e481–e492.
17. Lanzillotta M, Culver E, Sharma A, et al. Fibrotic phenotype of IgG4-related disease. *Lancet Rheumatol.* 2024;6:e469–e480.
18. Röhrich M, Leitz D, Glatting FM, et al. Fibroblast activation protein-specific PET/CT imaging in fibrotic interstitial lung diseases and lung cancer: a translational exploratory study. *J Nucl Med.* 2022;63:127–133.
19. Perugino CA, Stone JH. IgG4-related disease: an update on pathophysiology and implications for clinical care. *Nat Rev Rheumatol.* 2020;16:702–714.
20. Iguchi T, Takaori K, Mii A, et al. Glucocorticoid receptor expression in resident and hematopoietic cells in IgG4-related disease. *Mod Pathol.* 2018;31:890–899.
21. Löhr JM, Vujasinovic M, Rosendahl J, Stone JH, Beuers U. IgG4-related diseases of the digestive tract. *Nat Rev Gastroenterol Hepatol.* 2022;19:185–197.
22. Peng L, Zhang X, Zhou J, et al. Comparison of clinical features and outcomes of proliferative, fibrotic, and mixed subtypes of IgG4-related disease: a retrospective cohort study. *Chin Med J (Engl).* 2024;137:303–311.